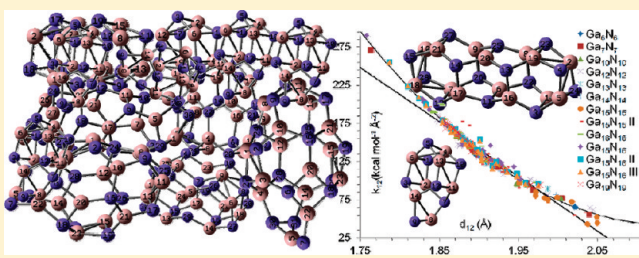


# Ab Initio Analysis and Harmonic Force Fields of Gallium Nitride Nanoclusters

Emily C. Perez-Angel<sup>†</sup> and Jorge M. Seminario<sup>\*,†,‡,§</sup><sup>†</sup>Department of Chemical Engineering, <sup>‡</sup>Materials Science and Engineering Graduate Program, and <sup>§</sup>Department of Electrical and Computer Engineering, Texas A&M University, College Station, Texas 77843, United States

**ABSTRACT:** Gallium nitride (GaN) clusters are analyzed to set approaches for more extended calculations at the nanoscale. We test the atom components and very small clusters using the most sophisticated compound methods such as G1–G3, CBS, W1, and a flavor of DFT (B3PW91) using several sizes and qualities of basis sets. Results are compared with very precise experimental information when available. Interestingly, the B3PW91 yields results comparable to the high-quality compound methods. For negative ions, it is difficult to assess the quality of the methods; the electron affinity (EA) calculations, as expected, yield better results when diffuse functions are used. All ionization potentials (IPs) are well reproduced by all methods, but the best results are obtained with B3PW91 for the Ga atom and with the compound methods for N. Among the compound methods, the W1 ones use the largest basis sets with 93 functions (which include two sets of  $g$ -functions) for one gallium atom. Geometry optimizations are performed with MP2 for the G-methods, HF for the CBS-methods (except QB3), and B3LYP for the CBS-QB3 and all W1 methods. G3 followed by B3PW91 yields the best result for the Ga quartet excited state, and there is little difference for the excited doublet of N, among the compound methods. In general all calculated IPs and EAs are in good agreement with existing experimental data. We also performed extended calculations of bigger GaN clusters such as  $\text{Ga}_x\text{N}_y$  where  $6 < x \approx y < 19$  using B3PW91/6-311G(d). Finally, we calculate second derivative and thus the vibrational spectra for all clusters studied. We generate harmonic force fields using the procedure *Fuerza* and averaged the force field parameters and use them in a simple heating molecular dynamics calculation that yields an acceptable value for the heat capacity.



**Table 1.** Compound Procedures Used in This Work, Their Highest Level Methods and Largest Basis Sets (In All Cases the Highest Methods Are Not Used with the Largest Basis Set), Methods Used for the Geometry Optimization, Specific Basis Set, and Number of Functions for Ga and N Highest Basis Sets

procedure	method	opt method	basis set	Ga basis	$n_{\text{Ga}}$	N basis	$n_{\text{N}}$
G1	QCISD(T,E4T)	MP2	6-311G(2df)	8s7p4d1f	56	1s3sp2d1f	30
G2	QCISD(T,E4T)	MP2	6-311+G(3df)	8s1sp7p5d1f	65	1s4sp3d1f	39
G3	QCISD(T,E4T)	MP2	GTLarge	8s1sp7p7d3f	89	1s4sp1p3d1f	42
CBS-4M	MP4SDQ	HF	CBSB1	8s1sp7p5d2f	72	1s4sp2d1f	34
CBS-QB3	CCSD(T)	B3LYP	CBSB3	8s1sp7p5d2f	72	1s4sp2d1f	34
CBS-APNO	CCSD(T)	HF	CBSB5	n/a	n/a	6s6p3d2f	53
W1U	CCSD(T)	B3LYP	aug-cc-pVQZ	8s7p5d3f2g	93	6s5p4d3f2g	80
W1BD	BD(T)	B3LYP	aug-cc-pVQZ	8s7p5d3f2g	93	6s5p4d3f2g	80
W1RO	CCSD(T)	B3LYP	aug-cc-pVQZ	8s7p5d3f2g	93	6s5p4d3f2g	80

GaN can be a useful material for transistors in power switching and millimeter-wave applications and microelectronic devices operating at high temperatures.<sup>9,11</sup> Recently, pure GaN crystals have revolutionized the electronics industry, making better violet lasers yields, allowing more controllable wavelength, and improving the optoelectronics industry. It is projectable that LEDs could perform better, replacing the century-old incandescent bulb, and be used also for efficient power-handling circuitry in hybrid electric vehicles.<sup>13</sup> Materials and devices made from or containing GaN have been extensively studied since the early 90s experimentally<sup>12</sup> and theoretically using ab initio electronic structure methods for GaN clusters.<sup>8,11,14–20</sup>

In this work, we calculate and compare to precise experimental results the excitation energies, ionization potentials (IP), and electron affinities (EA). IP and EA are calculated for Ga and N ions as well as the EA for the Ga<sub>2</sub>N molecule using the most sophisticated and precise methods in the theoretical chemistry arsenal. We also calculate small Ga<sub>x</sub>N<sub>y</sub> ( $x = 1–3$ ,  $y = 1–5$ ) clusters with neutral, positive, and negative charges, testing several possible geometrical conformations in their ground states. Dissociation energies ( $D_e$ ) are also calculated for the Ga<sub>x</sub>N<sub>y</sub> clusters as well as their IPs and EAs. Then, calculate 13 small Ga<sub>x</sub>N<sub>y</sub> ( $x = y = 6–19$ ) clusters with hexagonal wurtzite crystal geometries that thermodynamically are the more stable structures resembling bulk GaN.<sup>11,15</sup> Finally, we calculate force-field functions for GaN clusters and then use them to estimate the heat capacity of GaN.

## METHODOLOGY

Several methods have been developed for electronic structure calculations using traditional and DFT methods to solve the Bohr–Oppenheimer electronic time-independent Schrödinger equation,  $H\Psi = E\Psi$ , where  $E$  is the total system energy,  $\Psi$  the wave function, and  $H$  the Hamiltonian operator.<sup>21</sup> Though there is no, in practice, perfect ab initio method, they are classified as the traditional ab initio, such as those starting from a Hartree–Fock (HF) approach and improved with sophisticated corrections to the energy and wave function, and the DFT methods that prefer to use the electron density instead of the real wave function as the main variable. In the most popular DFT methods, an imaginary wave function of noninteracting electrons is used to describe an electron density identical to the one of the real system. Therefore, both approaches may use a Slater determinant of molecular orbitals (MOs) which in turn are

**Table 2.** Total Energies in Ha and Relative Energies ( $\Delta E$ ) in eV for the First Excited Quartet of the Neutral Ga Atom<sup>a</sup>

method	basis set	energy (Ha)	$\Delta E$ (eV)	error (eV)
B3PW91	6-31G(d)	-1922.67575	4.44	-0.27
B3PW91	6-31+G(d)	-1922.67873	4.44	-0.27
B3PW91	6-311G(d)	-1924.61896	4.52	-0.19
B3PW91	6-311+G(d)	-1924.61900	4.52	-0.19
B3PW91	aug-cc-pVDZ	-1924.62505	4.55	-0.16
B3PW91	aug-cc-pVTZ	-1924.69233	4.52	-0.19
B3PW91	aug-cc-pVQZ	-1924.69653	4.51	-0.20
B3PW91	aug-cc-pVSZ	-1924.70014	4.52	-0.19
G1		-1923.07621	4.20	-0.51
G2		-1923.08277	4.17	-0.54
G3		-1924.11475	4.63	-0.08
CBS-4M		-1923.16694	4.29	-0.42
CBS-QB3		-1923.34859	4.48	-0.23
expt. <sup>53</sup>			4.71	
expt. <sup>53</sup>			4.79	

<sup>a</sup>The ground state in all levels of theory is a doublet, and it is used as a reference. The first experimental energy corresponds to the  $J = 1/2$ , and the second one corresponds to the weighted average energy of all contributions to the quartet. Errors in eV correspond to the difference between the calculated value and the first experimental energy.

linear combinations of atomic-orbital-like functions (basis set) centered at the nuclei sites and with coefficients of the linear expansions solved by a self-consistent procedure.<sup>1</sup> This is done for the HF and for the DFT Hamiltonians.

In this work, GAUSSIAN-03<sup>22</sup> and GAUSSIAN-09<sup>23</sup> programs are used to calculate several GaN clusters using complete basis set (CBS) methods (CBS-4 M,<sup>24,25</sup> CBS-QB3,<sup>25,26</sup> and CBS-APNO<sup>24</sup>), Gaussian-1 to Gaussian-3 methods (G1,<sup>27,28</sup> G2,<sup>29</sup> and G3<sup>30</sup>), W1 methods<sup>31,32</sup> (W1U, W1BD, and W1RO), and the B3PW91 functional with several sizes of basis sets. The DFT B3PW91<sup>33</sup> hybrid functional includes the Becke-3 exchange<sup>34,35</sup> and the Perdew–Wang-91 correlation functional.<sup>36–38</sup> The basis sets used with B3PW91 are the 6-31G(d) and 6-31+G(d),<sup>39–46</sup> the 6-311G(d) and 6-311+G(d),<sup>42,46–48</sup> as well as the correlation-consistent (cc) including diffuse functions (aug):<sup>49,50</sup> aug-cc-pVDZ, aug-cc-pVTZ, aug-cc-pVQZ, aug-cc-pVSZ, and aug-cc-pV6Z.<sup>51,52</sup>

Table 1 shows the main characteristics of the compound methods used in this work. Under method, the most advanced method used by each procedure is indicated, and under basis set,

**Table 3.** Total Energies in Ha and Relative Energies ( $\Delta E$ ) in eV for the Lowest Doublet State of the Neutral N Atom for Several Levels of Theory<sup>a</sup>

method	basis set	energy (Ha)	$\Delta E$ (eV)	error (eV)
B3PW91	6-31G(d)	-54.44994	3.10	0.72
B3PW91	6-31+G(d)	-54.45539	3.02	0.64
B3PW91	6-311G(d)	-54.46488	3.06	0.68
B3PW91	aug-cc-pVDZ	-54.46180	3.02	0.64
B3PW91	6-311+G(d)	-54.46840	3.01	0.63
B3PW91	aug-cc-pVTZ	-54.47175	2.98	0.60
B3PW91	aug-cc-pVQZ	-54.47474	2.98	0.60
B3PW91	aug-cc-pVSZ	-54.47568	2.98	0.60
B3PW91	aug-cc-pV6Z	-54.47583	2.98	0.60
CBS-4M		-54.41394	2.98	0.60
G2		-54.42208	2.57	0.19
G1		-54.42293	2.54	0.16
CBS-QB3		-54.42421	2.58	0.20
G3		-54.46910	2.55	0.17
CBS-APNO		-54.48723	2.63	0.25
W1BD		-54.51173	2.67	0.29
W1RO		-54.51175	2.67	0.29
W1U		-54.51176	2.67	0.29
expt. <sup>53</sup>		2.38		

<sup>a</sup>The excitation energies ( $\Delta E$ ) are from the ground state quartet of the neutral N. The experimental energy corresponds to the  $J = 5/2$ , and the error in eV corresponds to the difference between the calculated value and experimental data.

**Table 4.** First, Second, and Third Ionization Potentials (IP1, IP2, IP3, Respectively) and Their Errors ( $\Delta$ ) from the Experimental Values of Ga (All Units Are in eV)<sup>a</sup>

method	basis set	IP1	$\Delta$ IP1	IP2	$\Delta$ IP2	IP3	$\Delta$ IP3
B3PW91	6-31G(d)	6.06	0.06	20.08	-0.42	30.74	0.03
B3PW91	6-31+G(d)	6.07	0.07	20.09	-0.42	30.74	0.03
B3PW91	6-311G(d)	6.07	0.07	20.25	-0.26	30.82	0.11
B3PW91	6-311+G(d)	6.07	0.07	20.25	-0.26	30.82	0.11
B3PW91	aug-cc-pVDZ	6.06	0.06	20.27	-0.24	30.84	0.13
B3PW91	aug-cc-pVTZ	6.07	0.08	20.24	-0.27	30.69	-0.02
B3PW91	aug-cc-pVQZ	6.06	0.06	20.18	-0.33	30.80	0.09
B3PW91	aug-cc-pVSZ	6.07	0.07	20.21	-0.30	30.82	0.11
G1		5.85	-0.15	19.64	-0.87	29.20	-1.50
G2		5.86	-0.14	19.61	-0.90	29.19	-1.52
G3		6.01	0.01	20.37	-0.14	30.16	-0.55
CBS-4M		5.93	-0.07	20.02	-0.49	29.60	-1.11
CBS-QB3		5.98	-0.02	20.25	-0.26	29.94	-0.77
expt. <sup>78</sup>		5.999		20.51		30.71	

<sup>a</sup>The ground states of Ga, Ga<sup>+1</sup>, Ga<sup>+2</sup>, and Ga<sup>+3</sup> are doublet, singlet, doublet, and singlet, respectively.

the largest basis set used is shown; however, these two, method and basis set, are not necessarily used simultaneously in the calculations. Also indicated in Table 1 are the methods used for the geometry optimizations. In addition, the type and size of the largest basis sets for Ga and N are also indicated. The CBSBS5 Ga basis set is not available; it is the largest basis set used in CBS-APNO. Geometry optimizations are performed with the MP2/6-31G(d)

**Table 5.** First, Second, and Third Ionization Potentials (IP1, IP2, IP3, Respectively) and Their Errors ( $\Delta$ ) from the Experimental Values of N (All Units Are in eV)<sup>a</sup>

method	basis set	IP1	$\Delta$ IP1	IP2	$\Delta$ IP2	IP3	$\Delta$ IP3
B3PW91	6-31G(d)	14.79	0.26	30.12	0.52	48.15	0.70
B3PW91	6-31+G(d)	14.83	0.30	30.07	0.47	48.12	0.67
B3PW91	6-311G(d)	14.77	0.23	30.01	0.41	48.14	0.69
B3PW91	6-311+G(d)	14.79	0.26	29.99	0.39	48.16	0.71
B3PW91	aug-cc-pVDZ	14.81	0.27	30.05	0.45	48.18	0.73
B3PW91	aug-cc-pVTZ	14.78	0.24	30.00	0.40	48.12	0.67
B3PW91	aug-cc-pVQZ	14.77	0.24	30.01	0.41	48.15	0.70
B3PW91	aug-cc-pVSZ	14.77	0.24	30.02	0.42	48.15	0.71
B3PW91	aug-cc-pV6Z	14.77	0.24	30.02	0.42	48.16	0.71
G1		14.47	-0.06	29.45	-0.15	47.25	-0.19
G2		14.48	-0.06	29.46	-0.14	47.27	-0.18
G3		14.51	-0.03	29.51	-0.09	47.32	-0.12
CBS-QB3		14.49	-0.04	29.48	-0.12	47.29	-0.15
CBS-4M		14.56	0.02	29.47	-0.13	47.22	-0.23
CBS-APNO		14.53	0.00	29.61	0.01	47.46	0.02
W1BD		14.54	0.01	29.60	-0.01	47.41	-0.04
W1RO		14.54	0.01	-	-	-	-
W1U		14.54	0.01	29.60	0.00	47.41	-0.04
expt. <sup>79</sup>		14.534		29.601		47.448	

<sup>a</sup>The ground states of N, N<sup>+1</sup>, N<sup>+2</sup>, and N<sup>+3</sup> are quartet, triplet, doublet, and singlet, respectively.

**Table 6.** Electron Affinities and Their Errors with Respect to the Experimental Value of Ga<sup>a</sup>

method	basis set	EA (eV)	error EA (eV)
B3PW91	6-31G(d)	0.06	-0.37
B3PW91	6-311G(d)	0.31	-0.12
B3PW91	6-31+G(d)	0.48	0.05
B3PW91	6-311+G(d)	0.48	0.05
B3PW91	aug-cc-pVTZ	0.45	0.02
B3PW91	aug-cc-pVQZ	0.47	0.04
B3PW91	aug-cc-pVSZ	0.47	0.04
G1		0.33	-0.09
G2		0.33	-0.10
G3		0.29	-0.14
CBS-QB3		0.34	-0.09
expt. <sup>80</sup>		0.43	

<sup>a</sup>The ground state of Ga and Ga<sup>-1</sup> are doublet and triplet, respectively.

level for G1–G3 methods; HF for CBS-4 M and CBS-APNO using 3-21G(d) and 6-311G(d,p), respectively; and B3LYP/cc-pVTZ+d for the W1-methods, and the B3LYP/6-311G(2d,d,p) level of theory is used for the CBS-QB3. The W1 methods use the largest basis sets.

## RESULTS AND DISCUSSION

Whenever predictive calculations are needed, a good idea is to test available related experimental information with the methodology being used, which is usually not of the highest level of theory but corresponds to some trade-off to be able to analyze relatively large systems. This also can provide us a good idea of

**Table 7. Electron Affinity (eV) and Errors (eV) with Respect to the Experiment for N<sup>a</sup>**

method	basis set	<i>E</i> (Ha)	EA (eV)	error EA (eV)
B3PW91	6-31G(d)	-54.50633	-1.57	-1.57
B3PW91	6-311G(d)	-54.53079	-1.26	-1.26
B3PW91	6-31+G(d)	-54.56451	0.02	0.02
B3PW91	6-311+G(d)	-54.57676	-0.01	-0.01
B3PW91	aug-cc-pVTZ	-54.58188	0.02	0.02
B3PW91	aug-cc-pVQZ	-54.58535	0.03	0.03
B3PW91	aug-cc-pVSZ	-54.58710	0.05	0.05
B3PW91	aug-cc-pV6Z	-54.58806	0.08	0.08
G1		-54.50623	-0.27	-0.27
G2		-54.50480	-0.32	-0.32
G3		-54.54937	-0.37	-0.37
CBS-QB3		-54.50917	-0.27	-0.27
CBS-4M		-54.51474	-0.24	-0.24
CBS-APNO		-54.55622	-0.75	-0.75
W1BD		-54.60331	-0.18	-0.18
W1RO		-54.60359	-0.17	-0.17
W1U		-54.60500	-0.13	-0.13
expt. <sup>81</sup>		0.00		

<sup>a</sup>The ground state of N and N<sup>-1</sup> are quartet and triplet, respectively.

**Table 8. Total Energies in Ha and D<sub>e</sub> in kcal/mol for the Ground State Neutral GaN Molecule That for Each Method Is a Triplet**

method	basis set	energy (Ha)	D <sub>e</sub> (kcal mol <sup>-1</sup> )	D <sub>e</sub> (eV)
B3PW91	6-31G(d)	-1977.48001	48.5	2.06
B3PW91	6-31+G(d)	-1977.48905	50.6	2.15
B3PW91	6-311G(d)	-1979.43710	47.0	2.00
B3PW91	6-311+G(d)	-1979.43947	47.4	2.02
B3PW91	aug-cc-pVDZ	-1979.43982	46.9	1.99
B3PW91	aug-cc-pVTZ	-1979.51932	50.1	2.13
B3PW91	aug-cc-pVQZ	-1979.52687	50.5	2.15
B3PW91	aug-cc-pVSZ	-1979.53171	50.4	2.15
G1		-1977.81919	45.3	1.96
G2		-1977.82209	43.6	1.89
G3		-1978.92450	48.2	2.09
CBS-QB3		-1978.11079	49.3	2.14
theor. <sup>82</sup>			2.08	
theor. <sup>82</sup>			1.99	

how much further we can go when better precision is required. On the basis of earlier calculations, we have used the B3PW91 functional with a relatively moderate basis set that allows us to easily reach systems with more than  $\sim 1000$  basis functions.

The first comparison that can be done with experiments using the highest levels of theory corresponds to the excitation energies to the lowest-energy states of the participating atoms. These excited states have different multiplicity from the one of the ground state of the atoms Ga and N in our particular case. For Ga (Table 2) the ground state is a doublet, thus we calculate the excitation energies to the lowest state of the quartet and compare them to precise experimental energies tabulated in the NIST web page,<sup>53</sup> which contains a variety of experimental information

**Table 9. Total Energies of Anions and Electron Affinity (EA) in eV for GaN<sup>a</sup>**

method	basis set	energy (Ha)	EA (eV)
B3PW91	6-31G(d)	-1977.53456	1.48
B3PW91	6-311G(d)	-1979.49488	1.57
B3PW91	6-31+G(d)	-1977.55140	1.70
B3PW91	6-311+G(d)	-1979.50213	1.71
B3PW91	aug-cc-pVDZ	-1979.50045	1.65
B3PW91	aug-cc-pVTZ	-1979.58119	1.68
B3PW91	aug-cc-pVQZ	-1979.58898	1.69
B3PW91	aug-cc-pVSZ	-1979.59400	1.70
G1		-1977.87991	1.65
G2		-1977.88112	1.61
G3		-1978.99515	1.92
CBS-QB3		-1978.18528	2.03

<sup>a</sup>The anion ground state found for all levels of theory is a doublet.

**Table 10. Total Energies in Ha and Electron Affinity (EA) in eV for Ga<sub>2</sub>N<sup>a</sup>**

method	basis set	energy (Ha)	EA (eV)	error EA (eV)
B3PW91	6-31G(d)	-3900.56802	2.30	-0.20
B3PW91	6-311G(d)	-3904.45852	2.34	-0.17
B3PW91	6-31+G(d)	-3900.58206	2.36	-0.15
B3PW91	6-311+G(d)	-3904.46151	2.37	-0.14
B3PW91	aug-cc-pVDZ	-3904.46402	2.36	-0.14
B3PW91	aug-cc-pVTZ	-3904.61498	2.33	-0.18
B3PW91	aug-cc-pVQZ	-3904.62673	2.32	-0.18
B3PW91	aug-cc-pVSZ	-3904.63540	2.33	-0.18
G1		-3901.29711	2.67	0.16
G2		-3901.30272	2.65	0.15
G3		-3903.45404	2.65	0.15
CBS-QB3		-3901.88163	2.61	0.10
expt. <sup>83</sup>			2.506	

<sup>a</sup>The ground state for each method is a singlet.

used in this work. Results in Table 2 clearly show that the B3PW91 functional using relatively small basis sets competes in quality with the most sophisticated compound methods. The best results are obtained for B3PW91/aug-cc-pVDZ.

Except for the G3 method, which yields an excellent agreement with the experiment, the B3PW91 with basis sets 6-31G(d) and 6-311G(d) yields better results than all the expensive G1, G2, and CBS-4 M methods, and it yields results similar to those from the CBS-QB3. This high quality of the B3PW91 is also consistent with the recent comparisons with experiment showing excellent reproduction of experimental electronic spectra.<sup>54,55</sup> Similar or related procedures using B3PW91 have been widely tested in the past with energetic materials,<sup>56–62</sup> molecular devices,<sup>63–65</sup> metallic clusters,<sup>66–69</sup> and combined procedures of molecular dynamics and DFT<sup>58,70</sup> calculations. DFT improves over HF-based calculations, which in the past provided good qualitative results,<sup>71,72</sup> and properties can be calculated from the wave function obtained solving the Schrödinger equation. This could be using density functional theory<sup>3,73,74</sup> or conventional wave function methods.<sup>75–77</sup> Further improvement of the basis set does not seem to reach further improvement in the

comparison with the experiment for this case. CBS-APNO and all W1 methods cannot be used with Ga because the CBSB6 basis set needed for CBS-APNO and the CC-pVTZ+d basis set required for all W1 methods are not available for Ga. In addition, the aug-cc-pV6Z is also not available for Ga.

We also calculate the excitation to the first sextet and octet of the Ga, for which there are not experimental excitation energies data available. We found that the best results for the sextet correspond to B3PW91/aug-cc-pV5Z, CBS-QB3, and G3 with

**Table 11.** Total Energies in Ha for Some  $\text{Ga}_x\text{N}_y$  Larger Clusters<sup>a</sup>

system	<i>q</i>	<i>m</i>	energy (Ha)
$\text{Ga}_6\text{N}_6$	0	1	-3900.56802
$\text{Ga}_7\text{N}_7$	0	1	-3904.45852
$\text{Ga}_{10}\text{N}_{10}$	0	1	-3900.58206
$\text{Ga}_{12}\text{N}_{12}$	0	1	-3904.46151
$\text{Ga}_{13}\text{N}_{13}$	0	1	-3904.46402
$\text{Ga}_{14}\text{N}_{14}$	0	1	-3904.61498
$\text{Ga}_{15}\text{N}_{15}$	0	1	-3904.62673
$\text{Ga}_{15}\text{N}_{15}$ II	0	1	-3904.63540
$\text{Ga}_{16}\text{N}_{16}$	0	1	-3901.29711
$\text{Ga}_{15}\text{N}_{16}$	0	2	-3901.30272
$\text{Ga}_{15}\text{N}_{16}$ II	-1	1	-3903.45404
$\text{Ga}_{15}\text{N}_{16}$ III	-3	1	-3901.88163
$\text{Ga}_{19}\text{N}_{19}$	0	1	-3900.56802

<sup>a</sup> *m* is the molecule multiplicity, and *q* is the charge. All geometries correspond to local minima. The hybrid B3PW91/6-31G(d) level of theory is used for the geometry optimizations. In the  $\text{Ga}_{16}\text{N}_{16}$  cluster, Ga8 (Figure 2) separates from the cluster, and thus the Ga was removed, creating three other clusters: one with neutral charge ( $\text{Ga}_{15}\text{N}_{16}$ ) and two more with negative charges, -1 and -3, corresponding to  $\text{Ga}_{15}\text{N}_{16}$  II and  $\text{Ga}_{15}\text{N}_{16}$  III, respectively.

excitation energies of 24.39, 24.14, and 24.66 eV, respectively. The agreement among the best levels of theory is excellent. It is found that the basis sets play an important role in the B3PW91 results. The octet results follow the same trend as the sextet, and the same conclusions can be drawn with energies of 57.39, 57.16, and 57.99 eV, respectively.

All compound methods, except the CBS-4M, yield better results than the DFT ones for the excitation energy from the ground state quartet of N to its first doublet state (Table 3). G1 and G3 yield the best results of all other methods with errors of 6.7 and 7.1%, respectively. All the W1 methods yield an error of 12%, and the CBS methods yield errors between the G1–G3 and W1 methods. On the other hand, the B3PW91 errors are in the range from 30 to 25%, slightly improving with the size of the basis set.

We also calculate the excitation energies to the sextet for which there is not experimental information; the results are certainly more unusual since the sextet would imply reaching the M shell for which none of the basis set provided is optimized. The following sequence of excitation energies is obtained: 16.2, 17.8, 17.8, and 18.4 eV for B3PW91, CBS-APNO, W1U, and G3, respectively.

The next tests correspond to the ionization potentials (IPs) of Ga and N. Table 4 shows the first three ionization potentials of Ga. For the first IP (IP1) all methods yield excellent results with errors smaller than 1.3% except for G1 and G2 with errors of 2.5 and 2.3%, respectively. The best fit to experiment corresponds again to the G3 with an error of only 0.01 eV (0.1%). The errors for the second (IP2) and third ionization potentials (IP3) are much larger than those for the IP1. G3 yields the best value for the IP2 with an error of 0.14 eV; all B3PW91 levels yield better results than G1, G2, and CBS-4M; and B3PW91 competes with CBS-QB3. However, for the IP3, all B3PW91 levels are better than any of the compound methods. Amazingly, for this IP3 the best results are obtained with B3PW91 using 6-31G(d) and 6-31G+(d) and also triple- and quadruple- $\zeta$  basis.

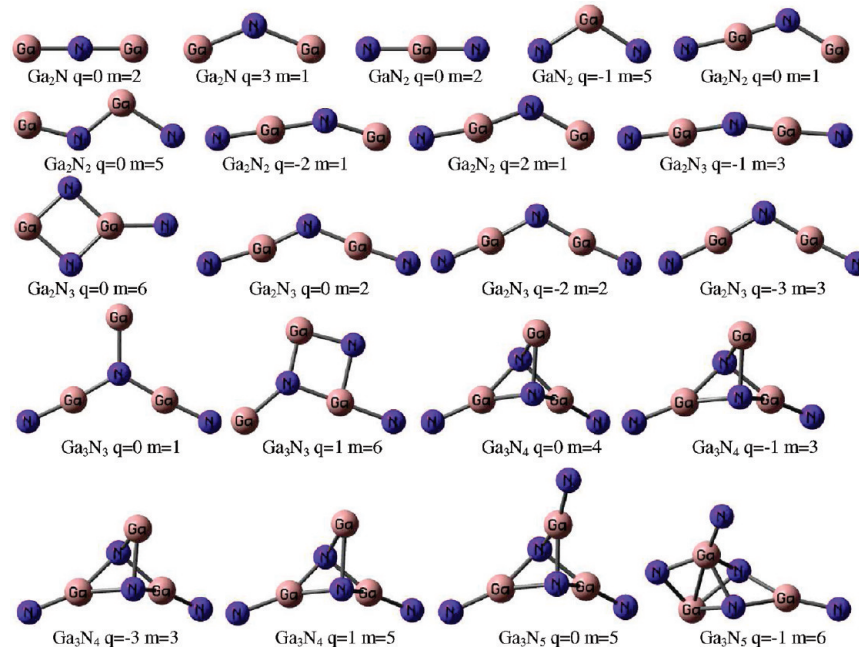


**Figure 1.** Some calculated GaN clusters: Ga (pink); N (purple); *q* is the charge; and *m* is the multiplicity, optimized with the hybrid B3PW91 functional. All geometries correspond to local minima.

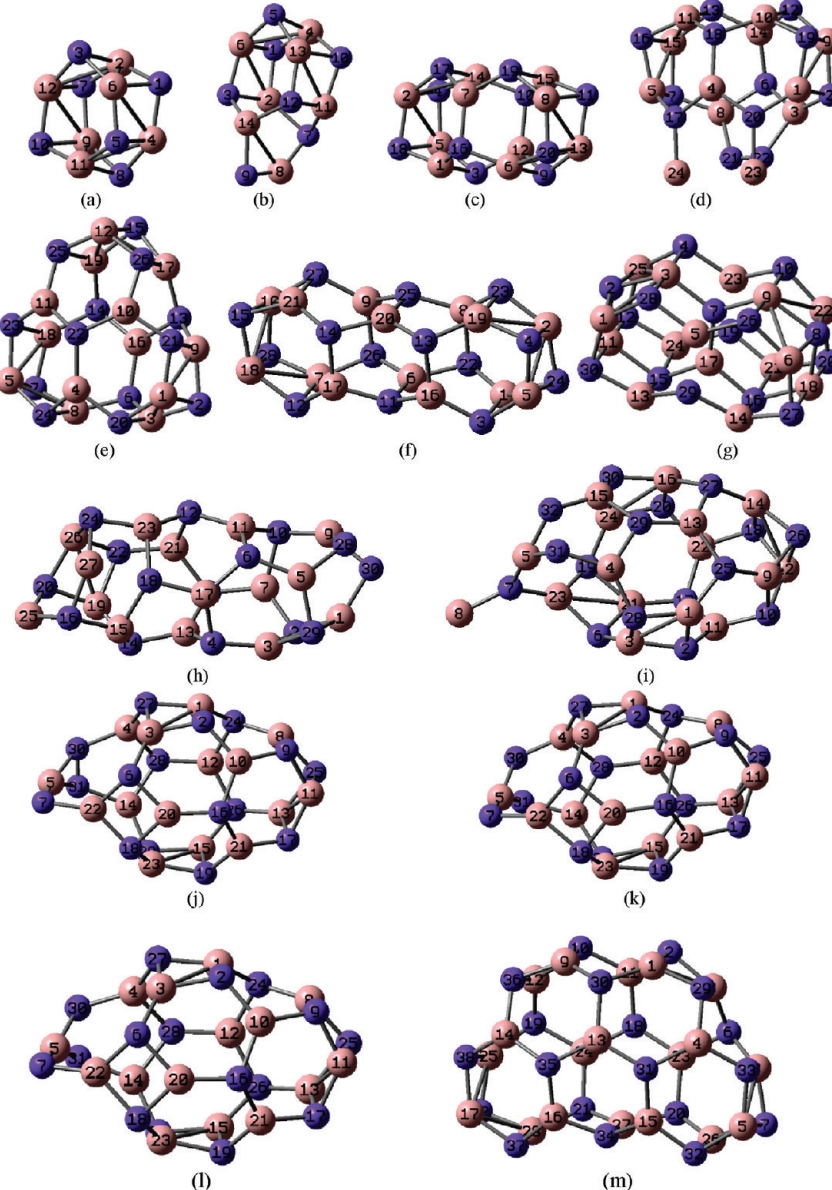


**Figure 2.** Clusters from Table 11 which correspond to local minima, where Ga is in light pink and N is in blue. The hybrid B3PW91 functional and 6-311G(d) basis set were used for the optimization: (a)  $\text{Ga}_6\text{N}_6$ , (b)  $\text{Ga}_7\text{N}_7$ , (c)  $\text{Ga}_{10}\text{N}_{10}$ , (d)  $\text{Ga}_{12}\text{N}_{12}$ , (e)  $\text{Ga}_{13}\text{N}_{13}$ , (f)  $\text{Ga}_{14}\text{N}_{14}$ , (g)  $\text{Ga}_{15}\text{N}_{15}$ , (h)  $\text{Ga}_{15}\text{N}_{15}$  II, (i)  $\text{Ga}_{16}\text{N}_{16}$ , (j)  $\text{Ga}_{15}\text{N}_{16}$ , (k)  $\text{Ga}_{15}\text{N}_{16}$  II, (l)  $\text{Ga}_{15}\text{N}_{16}$  III, (m)  $\text{Ga}_{19}\text{N}_{19}$ .

For the first three ionization potentials of N (Table 5), all compound methods yield better results than those of the DFT. For the IP1, errors of the compound methods range from 0.00 for the CBS-APNO to 0.06 eV, and the DFT levels errors range from 0.24 to 0.30 with the large basis set making no further improvement. For the IP2, the W1U and W1DB and CBS-APNO yield the best results practically reproducing the experimental results. They are followed by the G1–G3 methods and the other two CBS ones, all with errors between 0.09 and 0.15 eV. Then the B3PW91 method ranges from 0.39 to 0.52 eV errors. The W1RO compound method does not yield results for the IP2 and IP3 due perhaps to the incompatibility of the wave functions at the B3LYP and Hartree–Fock levels for the doublet  $\text{N}^{2+}$  and singlet  $\text{N}^{3+}$ . For the third IP, the errors with the B3PW91 are practically independent of the basis set, ranging from 0.67 to 0.71 eV. The

results obtained for the IP2 follow a trend very similar to those obtained with the IP1.

Our next quantity to check is the electron affinity (EA) of Ga and N. For Ga (Table 6) as expected the best results are obtained with diffuse functions; however, what was not expected is that DFT levels of B3PW91 provide much better results than the expensive compound methods. Also, the order of quality is reverse for the G1–G3 methods; usually, the G3 was almost in most cases better than the G1 and G2. Now the G1 and then the G2 are better than the G3. As it was explained before, CBS-APNO and W1 methods are not available for Ga and the aug-cc-pV6Z basis set. In addition, there are convergence problems with CBS-4 M for the triplet of the anion  $\text{Ga}^{-1}$ .

For the electron affinity of N (Table 7), results follow the trend observed in Table 6 for Ga. The best results are obtained

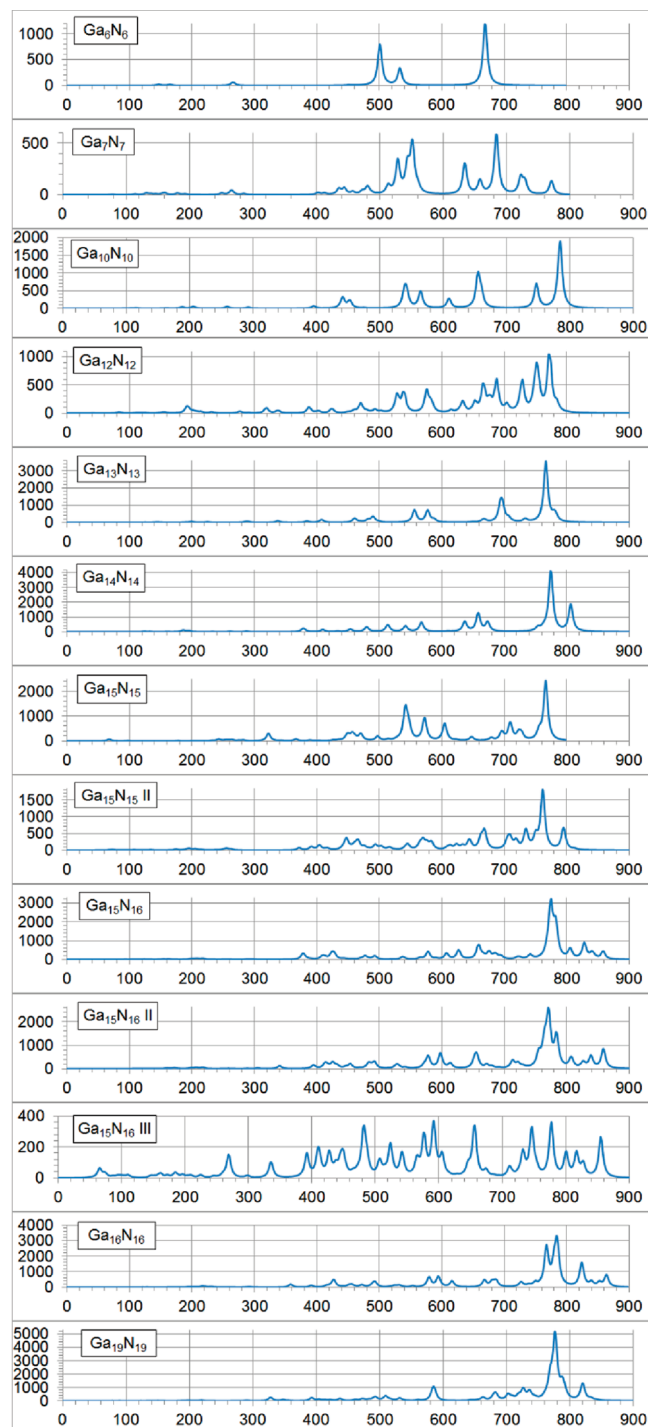


**Figure 3.** Vibrational IR spectra of the largest clusters. The horizontal axis is the frequency in  $\text{cm}^{-1}$ , and the vertical axis is the reflectivity. There is a peak after  $1500 \text{ cm}^{-1}$  for the  $\text{Ga}_{12}\text{N}_{12}$  cluster due to the  $\text{N21}-\text{N22}$  bond (see Figure 2(d)). This leaves the  $\text{Ga}_{23}$  and  $\text{Ga}_{24}$  dangling.

with the B3PW91 functional using small basis with diffuse functions; enlarging the basis set does not improve the EA further, and changing the level of theory only degrades the results. The error with the compound method is 1 order of magnitude larger than those using the B3PW91 with diffuse functions.

Our next analysis corresponds to the dissociation energies of small GaN related clusters. Although there is no experimental

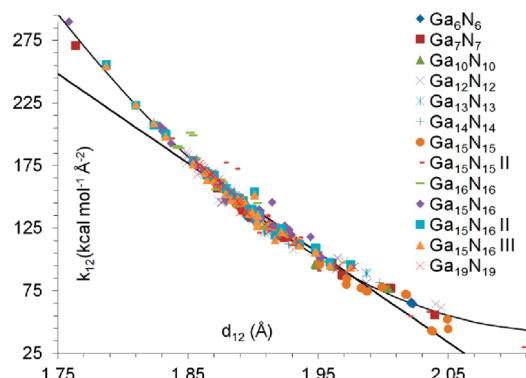


**Figure 4.** Relationship between Ga–N bond force constants ( $k_{12}$ ) in  $\text{kcal mol}^{-1} \text{\AA}^{-2}$  and their bond lengths ( $d_{12}$ ) in  $\text{\AA}$  of clusters from Table 11 and Figure 2:  $\text{Ga}_6\text{N}_6$ ,  $\text{Ga}_7\text{N}_7$ ,  $\text{Ga}_{10}\text{N}_{10}$ ,  $\text{Ga}_{12}\text{N}_{12}$ ,  $\text{Ga}_{13}\text{N}_{13}$ ,  $\text{Ga}_{14}\text{N}_{14}$ ,  $\text{Ga}_{15}\text{N}_{15}$ ,  $\text{Ga}_{15}\text{N}_{15}$  II,  $\text{Ga}_{16}\text{N}_{16}$ ,  $\text{Ga}_{15}\text{N}_{16}$  II,  $\text{Ga}_{15}\text{N}_{16}$  III,  $\text{Ga}_{19}\text{N}_{19}$ . The second-order polynomial approximation is  $k_{12} = 1693.4 \times (d_{12})^2 - 7237.8 \times d_{12} + 7776.3$  with a correlation factor of 0.9806. The lineal approximation is  $k_{12} = -715.04 \times d_{12} + 1499.7$  with a correlation factor of 0.9513. The average for Ga–N bond length is  $1.906 \text{ \AA}$  and for the force constant is  $136.7 \text{ kcal mol}^{-1} \text{\AA}^{-2}$ . The hybrid B3PW91 functional and 6-311G(d) basis set were used for the optimization and second derivative calculations. All regressions are performed using all data.

evidence on the GaN molecule, there are other theoretical data that were performed using CASSCF-MRSDCI/aug-cc-pVQZ with a calculated dissociation energy of 2.08 eV which is in good agreement with our results (Table 8), with discrepancies of only 0.01 up to 0.19 eV. All calculations seem to indicate that the molecule may exist; practically there are no major differences among the methods. Roughly at  $\sim 20 \text{ kcal/mol}$  is located the first excited state singlet of GaN, and the quintet is around the dissociation limit ( $\sim 0.3 \text{ kcal/mol}$ ). The effect of the zero-point vibrational energy is between 0.83 and 0.87 kcal/mol for all levels of theory, and it is considered in all calculations.

The  $\text{Ga}_2\text{N}$  is also calculated with a predicted dissociation energy of 136 and 139 kcal/mol with G1 and G2 methods in agreement with large basis set calculations with B3PW91/aug-cc-pVDZ (138 kcal/mol) and 151 kcal/mol with the CBS-QB3 in agreement with the B3PW91 results with small basis sets (152 and 154 kcal/mol) with double-z and double-z plus diffuse basis functions. The first excited quartet is  $\sim 72 \text{ kcal/mol}$ , and the values for the sextet are very inconclusive ( $\sim -1 \text{ kcal/mol}$ ). It also calculated the IP for this molecule; the first and second IPs for  $\text{Ga}_2\text{N}$  have values of  $\sim 8.0$  and  $\sim 19.0 \text{ eV}$ , respectively. Also, several combinations of charge and multiplicity were treated for  $\text{Ga}_2\text{N}$ , and their corresponding IP is also found using B3PW91 with not too large basis sets, mainly the 6-31G(d) and the 6-311(d).

Next, we calculate the first three IPs of  $\text{Ga}_2\text{N}$ . The first IP yields values of 8.1 eV assuming that the ground state of the first ion is a triplet; the singlet is very close in energy at 8.35 eV. The ionization to a quintet is  $\sim 11 \text{ eV}$ . For the second ionization potential, we get a value of 19 eV to the ground state quartet of the dication  $\text{Ga}_2\text{N}^+$ , and the IP to the doublet is 22.4 eV. All these values are obtained considering the results with the B3PW91 and the 6-31G(d) and 6-311G(d) basis sets.

For the  $\text{Ga}_2\text{N}_2$ , the first IP yields a precise value of 8.12 eV to the ground state doublet of the cation. The IP to the quartet is 8.13 eV, practically at the same energy as the doublet, and 9.6 to

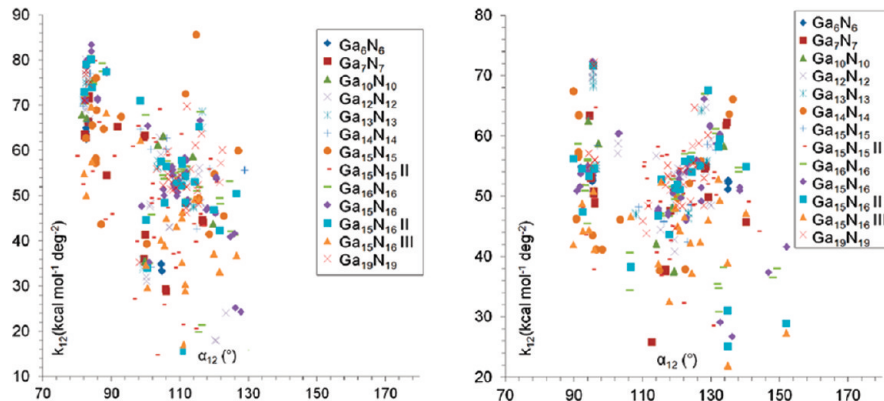


**Figure 5.** Relationship between angles ( $\alpha_{123}$ ) in degrees and their angle force constants ( $k_{123}$ ) in  $\text{kcal mol}^{-1} \text{deg}^{-2}$  of clusters from Table 11 and Figure 2:  $\text{Ga}_6\text{N}_6$ ,  $\text{Ga}_7\text{N}_7$ ,  $\text{Ga}_{10}\text{N}_{10}$ ,  $\text{Ga}_{12}\text{N}_{12}$ ,  $\text{Ga}_{13}\text{N}_{13}$ ,  $\text{Ga}_{14}\text{N}_{14}$ ,  $\text{Ga}_{15}\text{N}_{15}$ ,  $\text{Ga}_{15}\text{N}_{15}$  II,  $\text{Ga}_{16}\text{N}_{16}$ ,  $\text{Ga}_{15}\text{N}_{16}$  II,  $\text{Ga}_{15}\text{N}_{16}$  III,  $\text{Ga}_{19}\text{N}_{19}$ . The hybrid B3PW91 functional and 6-311G(d) basis set were used for the optimization. Ga–N–Ga angles (left) have a force constant and an angle average of 55.4  $\text{kcal mol}^{-1} \text{deg}^{-2}$  and 102.1°, respectively. N–Ga–N angles (right) have a force constant and an angle average of 51.7  $\text{kcal mol}^{-1} \text{deg}^{-2}$  and 114.9°, respectively. Angle values of Ga–N–Ga and N–Ga–N below 90° and over 160° are eliminated to be located at the ends of the structure and also to not be representative with respect to experimental measurements of GaN crystal wurtzite structure that for angles which are all equal have a value between 109.24° and 109.70°.<sup>84</sup>

the sextet. The second IP is 23.2 eV to the triplet dication ground state and 25.2 to the first excited state singlet of the dication. For the  $\text{Ga}_2\text{N}_3$ , the IP to the ground state quintet of the cation is 7.87 eV, to the triplet is 8.45, and to the singlet is 12.43 eV.

Electron affinities calculated for GaN are shown in Table 9. Most of the methods containing diffuse functions yield practically the same results, 1.6–1.7 eV, except for the two best, which yield values of 1.9–2.0 eV. As no experimental information is available for this molecule, it is difficult to assess a good estimate, which could be ~1.7–1.9 eV.

The electron affinity results for  $\text{Ga}_2\text{N}$  are shown in Table 10. All B3PW91 levels of theory procedures underestimate the EA, and the G1, G2, and CBS-QB3 overestimate it. The CBS-QB3 method yields the closest calculated value with respect to experimental data, but in general, all calculations yield good results. Some B3PW91 local minima geometries of small GaN clusters are shown in Figure 1.

For the construction of larger clusters, we take a hexagonal wurtzite unit cell with the experimental bulk properties of  $a = 3.190 \text{ \AA}$ ,  $c = 5.189 \text{ \AA}$ , and  $u = 0.377 \text{ \AA}^{84}$  to build the inputs of the 13 GaN clusters of Table 11 and Figure 2. Second derivatives are calculated with the procedure *Fuerza*<sup>85</sup> for all clusters with the goal to create harmonic force constants for further use in MD simulations of clusters. The clusters vibrational spectra (Figure 3) show a systematic behavior thus we expect the force constants to follow a similar trend. The relationship between their bond force constants and bond lengths for the Ga–N bonds shows a clear linear tendency (Figure 4) with small quadratic character. The regression to the second degree yields correlation factors higher than 0.95. The average bond force constant is 136.7  $\text{kcal mol}^{-1} \text{\AA}^{-2}$  with a bond length average of 1.906  $\text{\AA}$ . As a reference, the bulk bond length is 1.95  $\text{\AA}$ .<sup>84,86</sup>

It is difficult to find a clear relationship between angles and their force constants for the Ga–N–Ga and N–Ga–N angles shown in Figure 5. The average Ga–N–Ga and N–Ga–N angles are 102.1° and 114.9°, respectively, and their force constants are 55.4 and 51.7  $\text{kcal mol}^{-1} \text{deg}^{-2}$  close enough to use a single value. Those force fields (FFs) of those clusters will be very useful to perform MD simulations.

As side results, we also obtain the vibrational IR spectra of all clusters (Figure 3). A well-defined trend of reflectivity peaks

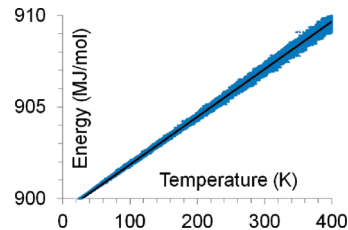


**Figure 6.** Energy versus temperature for the GaN crystal MD simulation using a cell 515 GaN pairs with periodic boundary conditions when a heating ramp from 0 to 400 K is applied. Blue points correspond to MD simulation, and the black line corresponds to the linear regression.

between the range of frequencies of 600 and 700  $\text{cm}^{-1}$  can be observed for  $\text{Ga}_6\text{N}_6$  and  $\text{Ga}_7\text{N}_7$  that are the smallest clusters, and a range between 700 and 800  $\text{cm}^{-1}$  is observed for the rest of the clusters. These results are in good agreement with reported results<sup>87</sup> of the measured infrared reflectivity at 300 K on GaN crystals using Kramers–Kronig technique; these results showed a clear peak tendency in the measurement of the reflectivity spectrum for the frequencies between 550 and 750  $\text{cm}^{-1}$ . The  $\text{Ga}_{12}\text{N}_{12}$  cluster has a N–N bond as observed in Figure 2, explaining a peak after 1500  $\text{cm}^{-1}$  (not shown).

To prove the force constants we obtained for Ga–N bonds and for Ga–N–Ga and N–Ga–N angles, we perform a MD simulation of a GaN crystal and determine its molar heat capacity ( $C_p$ ) with a parallelepiped unit cell of  $\sim 88,000 \text{ \AA}^3$  with 515 GaN pairs and 1873 Ga–N bonds with average length and force constant values of 1.906  $\text{\AA}$  and 136.7  $\text{kcal mol}^{-1} \text{\AA}^{-2}$ , respectively. The simulation considered 2544 Ga–N–Ga angles with their force constant values of 102.1° and 55.4  $\text{kcal mol}^{-1} \text{deg}^{-2}$ , respectively, and 2544 N–Ga–N angles and force constants with values of 114.9° and 51.7  $\text{kcal mol}^{-1} \text{deg}^{-2}$ , respectively. All these values for the constants correspond to averages from our DFT calculations. To quickly test if an acceptable range of results can be obtained without considering other contributions to the force field, we apply a heating ramp from 0 to 1300 K in 100 000 fs with a step time of 1 fs to the unit cell just described. Figure 6

shows that the behavior of the total energy versus the temperature may be approximated for the box by a linear regression with a correlation factor of 0.9988 where  $E (\text{J mol}^{-1}) = 26750T + 9 \times 10^8$ ; scaling with the 515 GaN pairs, we get

$$E (\text{J mol}^{-1}) = 51.94T + 1.75 \times 10^6 \quad (1)$$

Thus,  $C_p = 51.94 \text{ J mol}^{-1} \text{ K}^{-1}$  with a minimum value of 43.69  $\text{J mol}^{-1} \text{ K}^{-1}$ . An experimental molar heat capacity was measured for the range from 320 to 1270 K by calvet calorimetry and drop calorimetry methods with a temperature-dependent expression of the form<sup>88</sup>

$$\begin{aligned} C_p (\text{J mol}^{-1} \text{ K}^{-1}) &= 49.552 + 5.440 \times 10^{-3}T - 2.190 \\ &\times 10^6 T^{-2} + 2.460 \times 10^8 T^{-3} \end{aligned} \quad (2)$$

It was also measured by DSC method from 300 to 850 K yielding a temperature-dependent heat capacity<sup>89</sup>

$$\begin{aligned} C_p (\text{J mol}^{-1} \text{ K}^{-1}) &= 32.960 + 0.162 \\ &\times 10^{-1}T + 2360170T^{-2} - 775370000T^{-3} \end{aligned} \quad (3)$$

and a temperature-dependent heat capacity from 113 to 1073 K was also reported<sup>90</sup>

$$\begin{aligned} C_p (\text{J mol}^{-1} \text{ K}^{-1}) &= 30.310 + 25.203 \\ &\times 10^{-3}T - 285603T^{-2} - 6.523 \\ &\times 10^{-6}T^2 \end{aligned} \quad (4)$$

Thus, at 300 K, eqs 2, 3, and 4 yield heat capacities of 35.96, 35.33, and 34.11  $\text{J mol}^{-1} \text{ K}^{-1}$ , respectively. Comparing with the minimum value obtained from our simulation (43.69  $\text{J mol}^{-1} \text{ K}^{-1}$ ) using only the harmonic force field for bonds and angles, our estimated result is quite acceptable considering that at this point no other possible contributions to the total energy were considered. Usually force fields are fitted to reproduce physical properties.

## SUMMARY AND CONCLUSIONS

The hybrid B3PW91 functional with several basis sets (6-31G(d), 6-311G(d), 6-31+G(d), 6-311G+(d) and all the correlation-consistent basis sets with diffuse functions) yields results comparable to high-quality compound methods (G1-G3 methods, all CBS methods, and all W1 methods) with respect to existing experimental data. The B3PW91 with every basis set used performs well. G3 followed by B3PW91 yields the best result for the Ga quartet excitation energy. For N doublet excitation energy, the best results are given for all compound methods. All calculated IPs and EAs are in good agreement with existing experimental data. Electron affinity (EA) calculations for anions yield, certainly, better results when diffuse functions are used. All ionization potentials (IPs) are well reproduced by all methods, but the best results are obtained with B3PW91 for Ga cations and with all compound methods for N cations. The EA average error difference for Ga is  $\pm 0.1$  eV and for N is  $\pm 0.32$  eV. Also, the  $\text{Ga}_2\text{N}$  ( $\text{Ga}-\text{N}-\text{Ga}$ ) molecule has an average error difference for EA of  $\pm 0.16$  eV. The IR vibrational spectra are calculated for 13  $\text{Ga}_x\text{N}_y$  ( $6 < x, y < 19$ ) nanoclusters, optimized

with B3PW91/6-311G(d), which yields acceptable results when comparing with experimental data. The force field for the wurtzite GaN crystal is studied, beginning with the calculation of averages for bond and angle lengths and also for their respective force constants for the 13  $\text{Ga}_x\text{N}_y$  optimized clusters. Finally, the force field obtained from ab initio calculations is used in MD simulations, calculating the heat capacity of a GaN crystal, which yields a heat capacity consistent with experiment, even taking into account that the conditions and assumptions made for the MD simulation were not too sophisticated.

## ACKNOWLEDGMENT

We acknowledge financial support from the U.S. Defense Threat Reduction Agency DTRA through the U.S. Army Research Office, Project No. W91NF-06-1-0231, ARO/DURINT project # W91NF-07-1-0199, and ARO/MURI project # W91NF-11-1-0024.

## REFERENCES

- (1) Hehre, W. J. Ab initio molecular orbital theory. *Acc. Chem. Res.* **1976**, *9*, 399–406.
- (2) Kohn, W. Density Functional and Density Matrix Method Scaling Linearly with the Number of Atoms. *Phys. Rev. Lett.* **1996**, *76*, 3168–3171.
- (3) Kohn, W.; Sham, L. J. Self-Consistent Equations Including Exchange and Correlation Effects. *Phys. Rev.* **1965**, *140*, A1133.
- (4) Kohn, W.; Sham, L. J. Quantum Density Oscillations in an Inhomogeneous Electron Gas. *Phys. Rev.* **1965**, *137*, A1697.
- (5) Runge, E.; Gross, E. K. U. Density-Functional Theory for Time-Dependent Systems. *Phys. Rev. Lett.* **1984**, *52*, 997.
- (6) Maple, J. R.; Dinur, U.; Hagler, A. T. Derivation of force fields for molecular mechanics and dynamics from ab initio energy surfaces. *Proc. Natl. Acad. Sci. U.S.A.* **1988**, *85*, 5350–5354.
- (7) Edgar, J. H. *Properties of Group III Nitrides*; INSPEC, The Institution of Electrical Engineers: London, 1994.
- (8) Bungaro, C.; Rapcewicz, K.; Bernholc, J. Ab initio phonon dispersions of wurtzite AlN, GaN, and InN. *Phys. Rev. B* **2000**, *61*, 6720.
- (9) Simin, G.; Shur, M. S.; Gaska, R. Terminal THz GaN Based Transistors with Field and Space Charge Control Electrodes. *Int. J. High Speed Electron. Syst.* **2009**, *19*, 7–14.
- (10) Goldberger, J.; He, R.; Zhang, Y.; Lee, S.; Yan, H.; Choi, H.-J.; Yang, P. Single-crystal gallium nitride nanotubes. *Nature* **2003**, *422*, 599–602.
- (11) Lee, S. M.; Lee, Y. H.; Hwang, Y. G.; Lee, C. J. Electronic Structures of GaN Nanotubes. *J. Korean Phys. Soc.* **1999**, *34*, S253–S257.
- (12) Nakamura, S.; Senoh, M.; Iwasa, N.; Nagahama, S.-i. High-power InGaN single-quantum-well structure blue and violet light-emitting diodes. *Appl. Phys. Lett.* **1995**, *67*, 1868–1870.
- (13) Stevenson, R. The World's Best Gallium Nitride. *IEEE Spectrum* **2010**, *40*–45.
- (14) Nord, J.; Albe, K.; Erhart, P.; Nordlund, K. Modelling of compound semiconductors: analytical bond-order potential for gallium, nitrogen and gallium nitride. *J. Phys.: Condens. Matter* **2003**, *15*, 5649–5662.
- (15) Fritsch, J.; Sankey, O. F.; Schmidt, K. E.; Page, J. B. Ab initio calculation of the stoichiometry and structure of the (0001) surfaces of GaN and AlN. *Phys. Rev. B* **1998**, *57*, 15360.
- (16) Karch, K.; Wagner, J. M.; Bechstedt, F. Ab initio study of structural, dielectric, and dynamical properties of GaN. *Phys. Rev. B* **1998**, *57*, 7043.
- (17) Costales, A.; Pandey, R. Density Functional Calculations of Small Anionic Clusters of Group III Nitrides. *J. Phys. Chem. A* **2003**, *107*, 191–197.

- (18) Song, B.; Yao, C.-H.; Cao, P.-L. Density-functional study of structural and electronic properties of  $\text{Ga}_n\text{N}$  ( $n=1-19$ ) clusters. *Phys. Rev. B* **2006**, *74*, 035306.
- (19) Song, B.; Cao, P.-L. Geometric and electronic structures of small  $\text{GaN}$  clusters. *Phys. Lett. A* **2004**, *328*, 364–374.
- (20) Zhao, J.; Wang, B.; Zhou, X.; Chen, X.; Lu, W. Structure and electronic properties of medium-sized  $\text{Ga}_n\text{N}_n$  clusters ( $n = 4-12$ ). *Chem. Phys. Lett.* **2006**, *422*, 170–173.
- (21) Szabo, A.; Ostlund, N. S. *Modern Quantum Chemistry*; Dover Publications: New York, 1996.
- (22) Frisch, M. J.; Trucks, G. W.; Schlegel, H. B.; Scuseria, G. E.; Robb, M. A.; Cheeseman, J. R.; Montgomery, J. A., Jr.; Vreven, T.; Kudin, K. N.; Burant, J. C.; Millam, J. M.; Iyengar, S. S.; Tomasi, J.; Barone, V.; Mennucci, B.; Cossi, M.; Scalmani, G.; Rega, N.; Petersson, G. A.; Nakatsuji, H.; Hada, M.; Ehara, M.; Toyota, K.; Fukuda, R.; Hasegawa, J.; Ishida, M.; Nakajima, T.; Honda, Y.; Kitao, O.; Nakai, H.; Klene, M.; Li, X.; Knox, J. E.; Hratchian, H. P.; Cross, J. B.; Bakken, V.; Adamo, C.; Jaramillo, J.; Gomperts, R.; Stratmann, R. E.; Yazyev, O.; Austin, A. J.; Cammi, R.; Pomelli, C.; Ochterski, J. W.; Ayala, P. Y.; Morokuma, K.; Voth, G. A.; Salvador, P.; Dannenberg, J. J.; Zakrzewski, V. G.; Dapprich, S.; Daniels, A. D.; Strain, M. C.; Farkas, O.; Malick, D. K.; Rabuck, A. D.; Raghavachari, K.; Foresman, J. B.; Ortiz, J. V.; Cui, Q.; Baboul, A. G.; Clifford, S.; Cioslowski, J.; Stefanov, B. B.; Liu, G.; Liashenko, A.; Piskorz, P.; Komaromi, I.; Martin, R. L.; Fox, D. J.; Keith, T.; Al-Laham, M. A.; Peng, C. Y.; Nanayakkara, A.; Challacombe, M.; Gill, P. M. W.; Johnson, B.; Chen, W.; Wong, M. W.; Gonzalez, C.; Pople, J. A. *Gaussian 03*, revision C.02; Gaussian, Inc.: Wallingford, CT, 2004.
- (23) Frisch, M. J.; Trucks, G. W.; Schlegel, H. B.; Scuseria, G. E.; Robb, M. A.; Cheeseman, J. R.; Scalmani, G.; Barone, V.; Mennucci, B.; Petersson, G. A.; Nakatsuji, H.; Caricato, M.; Li, X.; Hratchian, H. P.; Izmaylov, A. F.; Bloino, J.; Zheng, G.; Sonnenberg, J. L.; Hada, M.; Ehara, M.; Toyota, K.; Fukuda, R.; Hasegawa, J.; Ishida, M.; Nakajima, T.; Honda, Y.; Kitao, O.; Nakai, H.; Vreven, T.; Montgomery, J.; J. A.; Peralta, J. E.; Ogliaro, F.; Bearpark, M.; Heyd, J. J.; Brothers, E.; Kudin, K. N.; Staroverov, V. N.; Kobayashi, R.; Normand, J.; Raghavachari, K.; Rendell, A.; Burant, J. C.; Iyengar, S. S.; Tomasi, J.; Cossi, M.; Rega, N.; Millam, N. J.; Klene, M.; Knox, J. E.; Cross, J. B.; Bakken, V.; Adamo, C.; Jaramillo, J.; Gomperts, R.; Stratmann, R. E.; Yazyev, O.; Austin, A. J.; Cammi, R.; Pomelli, C.; Ochterski, J. W.; Martin, R. L.; Morokuma, K.; Zakrzewski, V. G.; Voth, G. A.; Salvador, P.; Dannenberg, J. J.; Dapprich, S.; Daniels, A. D.; Ö. Farkas, Foresman, J. B.; Ortiz, J. V.; Cioslowski, J.; Fox, D. J. *Gaussian 09*, revision A.02; CT, W., Ed.; Gaussian, Inc., 2009.
- (24) Ochterski, J. W.; Petersson, G. A.; Montgomery, J. A. A complete basis set model chemistry. V. Extensions to six or more heavy atoms. *J. Chem. Phys.* **1996**, *104*, 2598.
- (25) Montgomery, J. A.; Frisch, M. J.; Ochterski, J. W.; Petersson, G. A. A complete basis set model chemistry. VII. Use of the minimum population localization method. *J. Chem. Phys.* **2000**, *112*, 11.
- (26) Montgomery, J. A.; Frisch, M. J.; Ochterski, J. W.; Petersson, G. A. A complete basis set model chemistry. VI. Use of density functional geometries and frequencies. *J. Chem. Phys.* **1999**, *110*, 6.
- (27) Pople, J. A.; Head-Gordon, M.; Fox, D. J.; Raghavachari, K.; Curtiss, L. A. Gaussian-1 theory: A general procedure for prediction of molecular energies. *J. Chem. Phys.* **1989**, *90*, 8.
- (28) Curtiss, L. A.; Jones, C.; Trucks, G. W.; Raghavachari, K.; Pople, J. A. Gaussian-1 theory of molecular energies for second-row compounds. *J. Chem. Phys.* **1990**, *93*, 9.
- (29) Curtiss, L. A.; Raghavachari, K.; Trucks, G. W.; Pople, J. A. Gaussian-2 theory for molecular energies of first- and second-row compounds. *J. Chem. Phys.* **1991**, *94*, 10.
- (30) Curtiss, L. A.; Raghavachari, K.; Redfern, P. C.; Rassolov, V.; Pople, J. A. Gaussian-3 (G3) theory for molecules containing first and second-row atoms. *J. Chem. Phys.* **1998**, *109*, 13.
- (31) Martin, J. M. L.; de Oliveira, G. Towards standard methods for benchmark quality ab initio thermochemistry-W1 and W2 theory. *J. Chem. Phys.* **1999**, *111*, 1843.
- (32) Parthiban, S.; Martin, J. M. L. Assessment of W1 and W2 theories for the computation of electron affinities, ionization potentials, heats of formation, and proton affinities. *J. Chem. Phys.* **2001**, *114*, 6014.
- (33) Becke, A. D. Density-functional thermochemistry. V. Systematic optimization of exchange-correlation functionals. *J. Chem. Phys.* **1997**, *107*, 8554.
- (34) Becke, A. D. Density-functional thermochemistry. IV. A new dynamical correlation functional and implications for exact-exchange mixing. *J. Chem. Phys.* **1996**, *104*, 1040.
- (35) Becke, A. D. Density-functional exchange-energy approximation with correct asymptotic behavior. *Phys. Rev. A* **1988**, *38*, 3098.
- (36) Perdew, J. P.; Burke, K.; Wang, Y. Generalized gradient approximation for the exchange-correlation hole of a many-electron system. *Phys. Rev. B* **1996**, *54*, 16533.
- (37) Perdew, J. P.; Burke, K.; Ernzerhof, M. Generalized Gradient Approximation Made Simple. *Phys. Rev. Lett.* **1996**, *77*, 3865.
- (38) Perdew, J. P.; Wang, Y. Accurate and simple analytic representation of the electron-gas correlation energy. *Phys. Rev. B* **1992**, *45*, 13244.
- (39) Hariharan, P. C.; Pople, J. A. The influence of polarization functions on molecular orbital hydrogenation energies. *Theor. Chem. Acc.* **1973**, *28*, 213–222.
- (40) Hehre, W.; Ditchfield, J. R.; Pople, J. A. Self-Consistent Molecular Orbital Methods. XII. Further Extensions of Gaussian-Type Basis Sets for Use in Molecular Orbital Studies of Organic Molecules. *J. Chem. Phys.* **1972**, *56*, 2257.
- (41) Rassolov, V. A.; Ratner, M. A.; Pople, J. A.; Redfern, P. C.; Curtiss, L. A. 6-31G\* basis set for third-row atoms. *J. Comput. Chem.* **2001**, *22*, 976–984.
- (42) Blaudeau, J.-P.; McGrath, M. P.; Curtiss, L. A.; Radom, L. Extension of Gaussian-2 (G2) theory to molecules containing third-row atoms K and Ca. *J. Chem. Phys.* **1997**, *107*, 5016.
- (43) Rassolov, V. A.; Pople, J. A.; Ratner, M. A.; Windus, T. L. 6-31G\* basis set for atoms K through Zn. *J. Chem. Phys.* **1998**, *109*, 1223.
- (44) Petersson, G. A.; Bennett, A.; Tensfeldt, T. G.; Al-Laham, M. A.; Shirley, W. A.; Mantzaris, J. A complete basis set model chemistry. I. The total energies of closed-shell atoms and hydrides of the first-row elements. *J. Chem. Phys.* **1988**, *89*, 2193.
- (45) Petersson, G. A.; Al-Laham, M. A. A complete basis set model chemistry. II. Open-shell systems and the total energies of the first-row atoms. *J. Chem. Phys.* **1991**, *94*, 6081.
- (46) Frisch, M. J.; Pople, J. A. J.; Binkley, S. Self-consistent molecular orbital methods 25. Supplementary functions for Gaussian basis sets. *J. Chem. Phys.* **1984**, *80*, 3265.
- (47) Wachters, A. J. H. Gaussian Basis Set for Molecular Wavefunctions Containing Third-Row Atoms. *J. Chem. Phys.* **1970**, *52*, 1033.
- (48) McGrath, M. P.; Radom, L. Extension of Gaussian-1 (G1) theory to bromine-containing molecules. *J. Chem. Phys.* **1991**, *94*, 511.
- (49) Kendall, R. A.; Dunning, J. T. H.; Harrison, R. J. Electron affinities of the first-row atoms revisited. Systematic basis sets and wave functions. *J. Chem. Phys.* **1992**, *96*, 6796–6806.
- (50) Woon, D. E.; Dunning, J. T. H. Gaussian basis sets for use in correlated molecular calculations. III. The atoms aluminum through argon. *J. Chem. Phys.* **1993**, *98*, 1358–1371.
- (51) Dunning, T. H. Gaussian basis sets for use in correlated molecular calculations. I. The atoms boron through neon and hydrogen. *J. Chem. Phys.* **1989**, *90*, 1007.
- (52) Wilson, A. K.; van Mourik, T.; Dunning, T. H. Gaussian basis sets for use in correlated molecular calculations. VI. Sextuple zeta correlation consistent basis sets for boron through neon. *J. Mol. Struct.: THEOCHEM* **1996**, *388*, 339–349.
- (53) Ralchenko, Y.; Kramida, A. E.; Reader, J. and NIST-ASD-Team. NIST Atomic Spectra Database (ver. 4.0.1) [Online]. Available: <http://physics.nist.gov/asd>
- (54) Fu, M.-L.; Adams, R. D.; Cristancho, D.; Leon, P.; Seminario, J. M. Spectroscopic and Photophysical Studies of Charge-transfer in a  $\text{Cd}_8$  thiolate cluster containing a coordinated N-Methyl-4,4-bipyridinium ligand. *Eur. J. Inorg. Chem.* **2011**, *2011*, 660–665.

- (55) Fu, M.-L.; Rangel, N. L.; Adams, R. D.; Seminario, J. M. Synthesis, Crystal Structure, Photophysical Properties, and DFT Calculations of a Bis(tetrathia-calix[4]arene) tetracadmium Complex. *J. Clust. Sci.* **2010**, *21*, 867–878.
- (56) Habibollahzadeh, D.; Grodzicki, M.; Seminario, J. M.; Politzer, P. Computational Study of the Concerted Gas-Phase Triple Dissociations of 1,3,5-Triazacyclohexane and its 1,3,5-Trinitro Derivative (RDX). *J. Phys. Chem.* **1991**, *95*, 7699–7702.
- (57) Politzer, P.; Seminario, J. M. Computational study of the structure of dinitraminic acid,  $\text{HN}(\text{NO}_2)_2$  and the energetics of some possible decomposition steps. *Chem. Phys. Lett.* **1993**, *216*, 348–352.
- (58) Seminario, J. M.; Concha, M. C.; Politzer, P. A Density Functional/Molecular Dynamics of the Structure of Liquid Nitromethane. *J. Chem. Phys.* **1995**, *102*, 8281–8282.
- (59) Politzer, P.; Seminario, J. M. Energy Changes Associated with Some Decomposition Steps of 1,3,3-Trinitroazetidine - a Nonlocal Density-Functional Study. *Chem. Phys. Lett.* **1993**, *207*, 27–30.
- (60) Politzer, P.; Seminario, J.; Bolduc, P. A Proposed Interpretation of the Destabilizing Effect of Hydroxyl-Groups on Nitroaromatic Molecules. *Chem. Phys. Lett.* **1989**, *158*, 463–469.
- (61) Seminario, J. M.; Concha, M. C.; Politzer, P. Calculated Structures and Relative Stabilities of Furoxan, some 1,2 Dinitrosoethylenes and other Isomers. *J. Comput. Chem.* **1992**, *13*, 177–182.
- (62) Murray, J.; Redfern, P.; Seminario, J.; Politzer, P. Anomalous Energy Effects in some Aliphatic and Alicyclic Aza Systems and their Nitro-Derivatives. *J. Phys. Chem.* **1990**, *94*, 2320–2323.
- (63) Seminario, J. M.; Araujo, R. A.; Yan, L. Negative Differential Resistance in Metallic and Semiconducting Clusters. *J. Phys. Chem. B* **2004**, *108*, 6915–6918.
- (64) Seminario, J. M.; De La Cruz, C.; Derosa, P. A.; Yan, L. Nanometer-Size Conducting and Insulating Molecular Devices. *J. Phys. Chem. B* **2004**, *108*, 17879–17885.
- (65) Derosa, P. A.; Guda, S.; Seminario, J. M. A programmable molecular diode driven by charge-induced conformational changes. *J. Am. Chem. Soc.* **2003**, *125*, 14240–14241.
- (66) Seminario, J. M.; Zacarias, A. G.; Castro, M. Systematic Study of the Lowest Energy States of Pd,  $\text{Pd}_2$ , and  $\text{Pd}_3$ . *Int. J. Quantum Chem.* **1997**, *61*, 515–523.
- (67) Seminario, J. M.; Tour, J. M. Systematic Study of the Lowest Energy States of  $\text{Au}_n$  ( $n=1–4$ ) Using DFT. *Int. J. Quantum Chem.* **1997**, *65*, 749–758.
- (68) Derosa, P. A.; Seminario, J. M.; Balbuena, P. B. Properties of Small Bimetallic Ni-Cu Clusters. *J. Phys. Chem. A* **2001**, *105*, 7917–7925.
- (69) Seminario, J. M.; Ma, Y.; Agapito, L. A.; Yan, L.; Araujo, R. A.; Bingi, S.; Vadlamani, N. S.; Chagarlamudi, K.; Sudarshan, T. S.; Myrick, M. L.; Colavita, P. E.; Franzon, P. D.; Nackashi, D. P.; Cheng, L.; Yao, Y.; Tour, J. M. Clustering Effects on Discontinuous Gold Film nanoCells. *J. Nanosci. Nanotech.* **2004**, *4*, 907–917.
- (70) Seminario, J. M.; Derosa, P. A.; Cordova, L. E.; Bozard, B. H. A Molecular Device Operating at Terahertz Frequencies. *IEEE Trans. Nanotech.* **2004**, *3*, 215–218.
- (71) Choi, D.-S.; Huang, S.; Huang, M.; Barnard, T. S.; Adams, R. D.; Seminario, J. M.; Tour, J. M. Revised Structures of N-Substituted Dibromo-Substituted Pyrrole Derivatives and their Polymeric Products. Termaleimide Models with Low Optical Bandgaps. *J. Org. Chem.* **1998**, *63*, 2646–2655.
- (72) Murray, J. S.; Seminario, J. M.; Politzer, P. Does Antiaromaticity Imply Net Destabilization. *Int. J. Quantum Chem.* **1994**, *49*, 575–579.
- (73) Hohenberg, P.; Kohn, W. Inhomogeneous Electron Gas. *Phys. Rev.* **1964**, *136*, B864.
- (74) Sham, L. J.; Kohn, W. One-Particle Properties of an Inhomogeneous Interacting Electron Gas. *Phys. Rev.* **1966**, *145*, 561.
- (75) Murray, J. S.; Peralta-Inga, Z.; Politzer, P.; Ekanayake, K.; LeBreton, P. Computational characterization of nucleotide bases: Molecular surface electrostatic potentials and local ionization energies, and local polarization energies. *Internat. J. Quantum Chem.* **2001**, *83*, 245–254.
- (76) Politzer, P.; Seminario, J. M. Relative bond strengths in tetrahedrane, prismane, and some of their aza analogs. *Struct. Chem.* **1990**, *1*, 29–32.
- (77) Scrocco, E.; Tomasi, J. The electrostatic molecular potential as a tool for the interpretation of molecular properties. *New Concepts II* **1973**, *95*–170.
- (78) Moerlein, S. M.; Welch, M. J. The chemistry of gallium and indium as related to radiopharmaceutical production. *Int. J. Nuclear Med. Biol.* **1981**, *8*, 277–287.
- (79) K. Barbalace. (1995 - 2010, 9/21/2010). *Periodic Table of Elements - Nitrogen - N*. Available: <http://EnvironmentalChemistry.com/yogi/periodic/N.html>
- (80) Williams, W. W.; Carpenter, C.; D L A M; Koepnick, M. C.; Calabrese, D.; Thompson, J. S. Laser photodetachment electron spectrometry of Ga. *J. Phys. B: At., Mol. Opt. Phys.* **1998**, *31*, L341–345.
- (81) Chen, E. C. M.; Chen, E. S. Molecular electron affinities and the calculation of the temperature dependence of the electron-capture detector response. *J. Chromatogr. A* **2004**, *1037*, 83–106.
- (82) Ueno, L. T.; Roberto-Neto, O.; Canuto, S.; Machado, F. B. C. The low-lying electronic states of the GaN molecule. *Chem. Phys. Lett.* **2005**, *413*, 65–70.
- (83) Sheehan, S. M.; Meloni, G.; Parsons, B. F.; Wehres, N.; Neumark, D. M. Spectroscopic characterization of the ground and low-lying electronic states of  $\text{Ga}_2\text{N}$  via anion photoelectron spectroscopy. *J. Chem. Phys.* **2006**, *124*, 064303–7.
- (84) Schulz, H.; Thiemann, K. H. Crystal structure refinement of AlN and GaN. *Solid State Commun.* **1977**, *23*, 815–819.
- (85) Seminario, J. M. Calculation of intramolecular force fields from second-derivative tensors. *Int. J. Quantum Chem.* **1996**, *60*, 1271–1277.
- (86) Das, G. P.; Rao, B. K.; Jena, P. Ferromagnetism in Mn-doped GaN: From clusters to crystals. *Phys. Rev. B* **2003**, *68*, 035207.
- (87) Barker, A. S.; Ilegems, M. Infrared Lattice Vibrations and Free-Electron Dispersion in GaN. *Phys. Rev. B* **1973**, *7*, 743.
- (88) Leitner, J.; Strejc, A.; Sedmidubský, D.; Ruzicka, K. High temperature enthalpy and heat capacity of GaN. *Thermochim. Acta* **2003**, *401*, 169–173.
- (89) Zięborak-Tomaszkiewicz, I.; Utzig, E.; Gierycz, P. Heat capacity of crystalline GaN. *J. Therm. Anal. Calorim.* **2008**, *91*, 329–332.
- (90) Chen, X.-I. Structure and Heat Capacity of Wurtzite GaN from 113 to 1073 K. *Chin. Phys. Lett.* **1999**, *16*, 107.